

Surface Structures and Conductance at Epitaxial Growths of Ag and Au on the Si(111) Surface

Shuji Hasegawa and Shozo Ino

Department of Physics, Faculty of Science, University of Tokyo, Hongo, Bunkyo-ku, Tokyo 113, Japan

(Received 16 December 1991)

In situ measurements of surface conductance, combined with simultaneous observations of reflection high-energy electron diffraction, clearly demonstrated strong dependence of the conductance on substrate-surface structures and epitaxial growth styles at early stages of Ag and Au depositions on Si(111) surface at room temperature. The conductance showed a large change with a small amount of deposition (<0.1 monolayer) on the substrate of a metal-induced superstructure ($\sqrt{3}\times\sqrt{3}$ -Ag or 5×2 -Au), while it scarcely changed for a clean 7×7 substrate. The results are discussed in terms of the Fermi-level pinning and space-charge layers.

PACS numbers: 73.25.+i, 61.14.Hg, 68.55.Jk

Clean and metal-covered semiconductor surfaces have been intensively investigated, for fundamental as well as practical interests, with a variety of surface-sensitive techniques such as electron diffraction, microscopy, and spectroscopy [1,2]. These methods have not only provided diversified information on the structures at atomic scales, but also have become indispensable tools to precisely control epitaxy, leading to fabrication of novel microelectronics devices. It has become, then, of great importance to simultaneously investigate both the atomic structures and various properties (electrical, optical, and magnetic) of surface regions. In spite of a great number of studies on the electrical properties of the semiconductor surfaces [3], it was not until recently that much attention was paid to the relationship between the properties and the atomic structures. The Schottky-barrier height at epitaxial $\text{NiSi}_2/\text{Si}(111)$ contacts was found by Tung to be strongly influenced by the atomic structure of the interface [4]. Heslinga *et al.* also demonstrated that the barrier heights of two types of contacts, $\text{Si}(111)\text{-}7\times 7\text{-Pb}$ and $\text{Si}(111)\text{-}\sqrt{3}\times\sqrt{3}\text{-Pb}$, are quite different [5]. Jałochowski and Bauer measured the electrical resistivity of thin metal films grown on a Si(111) surface with simultaneous observation of the reflection high-energy electron diffraction (RHEED) intensity oscillations, to investigate size effects [6].

This Letter describes our *in situ* observations on the changes both in atomic structures and in surface conductance at the initial epitaxial growths of Ag and Au films on the Si(111) surface. While monitoring the structural changes with RHEED during metal deposition, the conductance parallel to the surface was simultaneously measured. The conductance was found to show characteristic changes depending on the substrate-surface structures and epitaxial growth styles of the films. The growth mechanisms of Ag on a clean 7×7 surface at room temperature (RT) were found to be quite different from those on a $\sqrt{3}\times\sqrt{3}$ -Ag surface, resulting in remarkable differences in conductance changes. The conductance changes for the Au case were also strongly affected by the initial substrate surfaces, clean 7×7 or 5×2 -Au. These

variations may be attributed to changes in surface space-charge layers, and in conduction through inhomogeneous metal films. In contrast with the studies in the literature on alkali-metal-covered Si surfaces [7] and gas-adsorbed Ge and Si surfaces [8], the present study has the advantage of measuring the conductance with simultaneous structure analysis during metal deposition in a 10^{-10} -Torr environment.

An *n*-type Si(111) wafer of 48–50 Ωcm resistivity and $25\times 4\times 0.4\text{ mm}^3$ size was mounted on a pair of Ta rods and clamped with Ta plates (Fig. 1). Before each measurement run, the surface was cleaned to obtain a clear 7×7 RHEED pattern, by several flash heatings up to 1500 K for 5 sec with a direct current of 9.5 A through the Ta rod electrodes, followed by cooling after the current was turned off. The conductance near the surface region, under isothermal conditions at RT, was measured as a voltage drop between a pair of Ta wire contacts (0.4 mm in diameter) about 6 mm apart, kept in contact with the wafer by elasticity, with a constant current of 10 μA

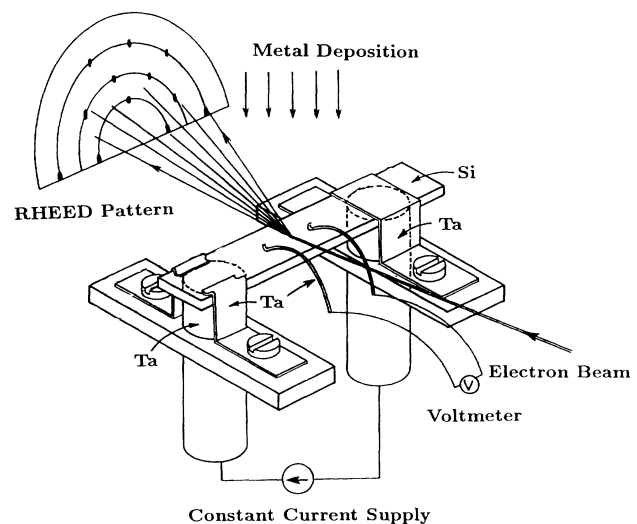


FIG. 1. The sample holder, drawn upside down.

supplied through the Ta rod electrodes. The heat treatments for cleaning with the Ta wires in contact made their contact resistance small and steady. A linear relation in the current-voltage characteristics was confirmed in the range from -1 to 1 mA with 0 V at 0 A. The structural changes of the surface between the pair of Ta wire contacts could be simultaneously analyzed with RHEED of 15 kV acceleration. Ag and Au were evaporated from alumina-coated W baskets which were placed about 50 cm away from the Si substrate. The amount of deposited material, expressed here in units of ML (monolayer, $1 \text{ ML} = 7.8 \times 10^{14}$ atoms/cm²), was monitored with a quartz-crystal oscillator. Since the primary beam of about $1 \mu\text{A}$ in RHEED disturbed the voltage between the Ta wire contacts, the beam was always turned off during the measurement, except for the intermittent observations of the RHEED patterns in the course of metal deposition.

Figure 2 shows the surface resistance changes, which are indicated as voltage drops between the Ta wire contacts, during Ag deposition (rate: 0.45 ML/min) at RT onto the clean 7×7 surface [Fig. 2(a)] and onto the $\sqrt{3} \times \sqrt{3}$ -Ag surface [Fig. 2(b)]. The RHEED patterns observed at the points indicated by arrows on the curves are shown as insets [Figs. 2(c)-2(f)]. The change in resistance in Fig. 2(a) was very small until the 7×7 pattern disappeared, with the exception of a slight increase at the beginning. In response to the subsequent development of a texture structure [Fig. 2(c)] of the Ag film, the resistance began to decrease steeply. This Ag film is known to grow in quasi-layer-by-layer fashion, consisting of twinning two-dimensional (2D) Ag crystals [9]. The phenomenon, on the other hand, seems rather different during deposition onto the $\sqrt{3}$ surface [Fig. 2(b)]. The resistance measurement was carried out at RT after cooling down from 670 K , at which the $\sqrt{3}$ structure [Fig. 2(d)] had been prepared on the substrate with 1-ML-Ag coverage [10]. After an abrupt decrease in resistance at the beginning, it decreases at a small rate. A ring pattern, with some preferential spots from Ag crystals, gradually emerged in the RHEED pattern with deposition, while the clear $\sqrt{3}$ pattern remained to the end [Figs. 2(e) and 2(f)]. This means that Ag atoms nucleate in three-dimensional (3D) form on the surface and scarcely cover the substrate surface [11] due to a high surface diffusivity of Ag adatoms on the $\sqrt{3}$ surface.

The resistance abruptly increased after the evaporator shutter was closed in Fig. 2(b), suggesting an influence of radiation from the Ag evaporator. However, radiation from the same type of empty evaporator, placed near the Ag evaporator and heated up to the same temperature, scarcely changed the resistance, as shown in Fig. 3 (periods *a* and *c*). We can safely say, therefore, that it is the deposited Ag atoms that cause the resistance changes (periods *b* and *d*). The resistance increase after closing the shutter may correspond to a process of nucleation of

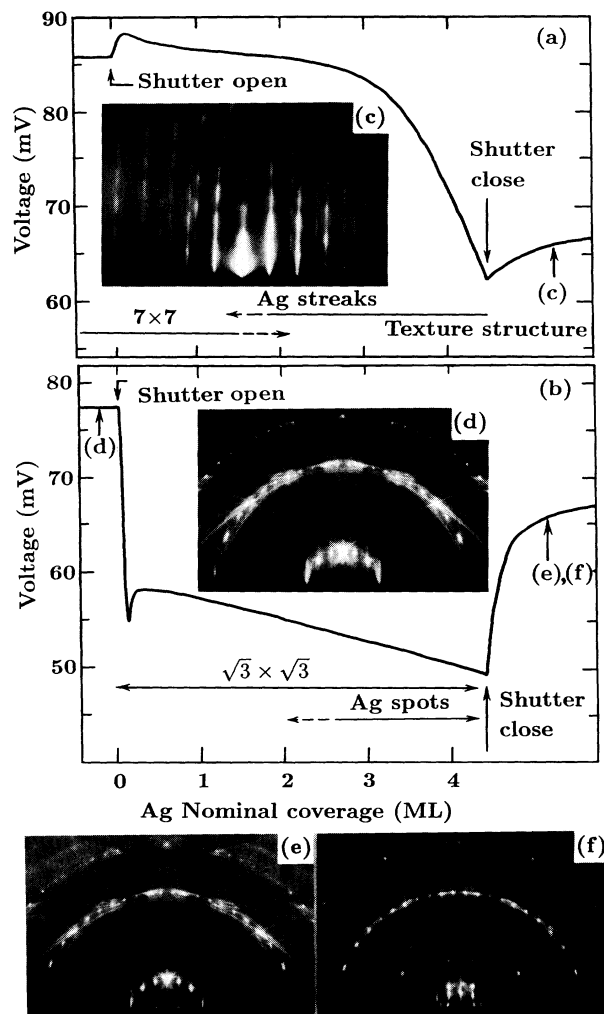


FIG. 2. The resistance changes during the room-temperature Ag depositions onto (a) clean Si(111)- 7×7 and (b) Si(111)- $\sqrt{3} \times \sqrt{3}$ -Ag surfaces. RHEED patterns are shown as insets: (c) a texture structure after 4.5-ML-Ag deposition on the 7×7 surface ($[1\bar{1}0]$ incidence); $\sqrt{3} \times \sqrt{3}$ -Ag substrate (d) before the Ag deposition ($[1\bar{1}2]$ incidence), (e) after 4.5-ML-Ag deposition onto (d), and (f) small glancing-angle observation of (e).

Ag adatoms on the $\sqrt{3}$ surface.

Figures 4(a) and 4(b) show the results of Au deposition (rate: 0.21 ML/min) at RT onto the Si(111)- 7×7 and -5×2 -Au surfaces, respectively. Compared with the Ag case, the initial voltages for each measurement before deposition were slightly scattered from one measurement run to another, probably because of interdiffusion of deposited Ag during heat treatments. The resistance in Fig. 4(a) does not show significant change at the initial deposition, except for a slight increase at the beginning, similar to the Ag case [Fig. 2(a)]. The subsequent decrease in resistance temporarily slows down around 2-ML-Au coverage, during which the 7×7 pattern [Fig. 4(d)] seems different from the clean one [Fig. 4(c)] in the intensity

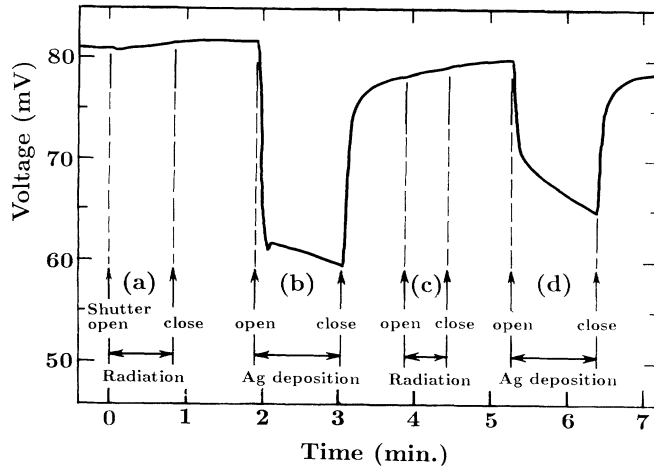


FIG. 3. The resistance for the Si(111)- $\sqrt{3}\times\sqrt{3}$ -Ag surface at room temperature scarcely changes during only thermal irradiation from an empty evaporator (periods *a* and *c*), but drastically changes during Ag deposition (rate: 1.6 ML/min) from another evaporator (periods *b* and *d*).

distribution of superlattice spots. On the other hand, after preparing the 5×2 structure [Fig. 4(e)] at 770 K by Au deposition of about 0.5 ML [12], the substrate was cooled down to RT and the resistance was measured [Fig. 4(b)]. The remarkable feature in this case is an abrupt large increase at the beginning. The maximum resistance in this change corresponded to a minor change in the RHEED pattern; the streaks in the 5×2 structure [Fig. 4(e)] disappeared to convert to a 5×1 structure. Similar changes in resistance were observed for $\sqrt{3}\times\sqrt{3}$ -Au and 6×6 -Au substrates. The final RHEED patterns in both Figs. 4(a) and 4(b) were almost the same faint 1×1 , resulting in similar slopes in the resistance decreases, irrespective of different starting substrate surfaces, which contrasts with the Ag case (Fig. 2). We did not observe a recovery in resistance after the deposition was stopped, such as in Fig. 2(b).

Although a conclusive explanation for the resistance changes mentioned above is lacking at present, a reasonable guess is that the initial changes at low metal coverages can be attributed to changes in the surface space-charge layer of the substrate, and that the subsequent changes with increasing metal coverage are caused by conduction through the metals films.

The Fermi level at the surface will shift and the band bending will change upon adsorption of metal atoms, resulting in a change in carrier concentration near the surface [3]. Although the change in surface conductance is composed of the product of a mobility and an excess carrier concentration, the mobility change is probably not of prime importance in our case. The Fermi level at the Si(111)- 7×7 surface has been proved to be pinned at the middle of the band gap by an intrinsic surface state, a metallic state, originating from the dangling-bond state on the adatoms [13] of the dimer-adatom-stacking-fault

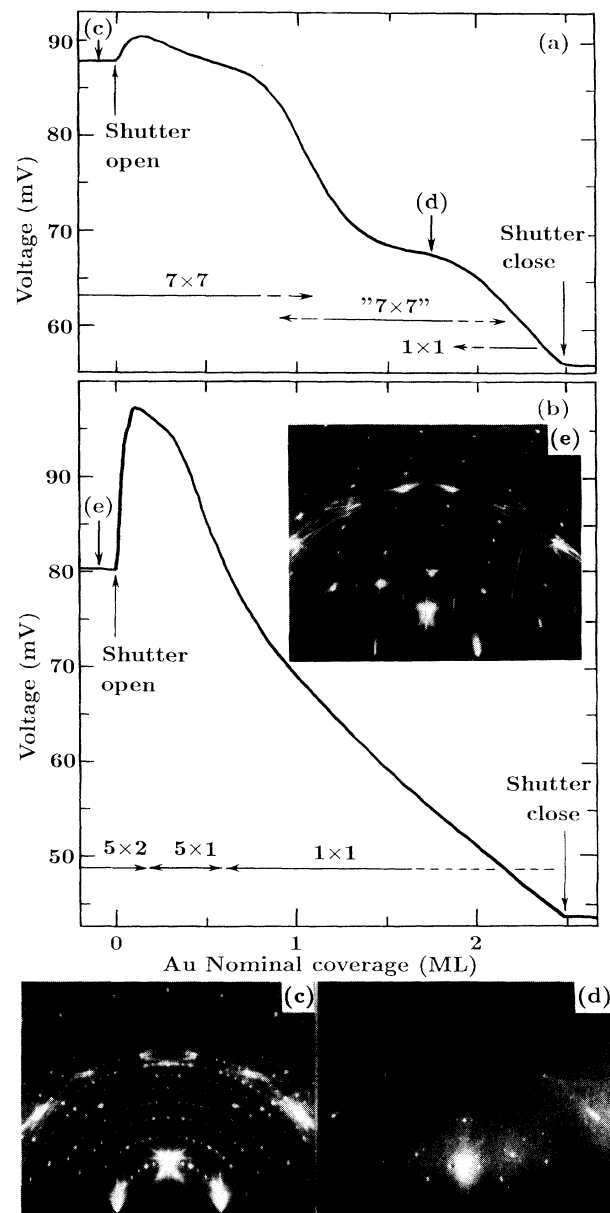


FIG. 4. The resistance changes during the room-temperature Au depositions onto (a) clean Si(111)- 7×7 and (b) Si(111)- 5×2 -Au surfaces. RHEED patterns are shown as insets: (c) the clean 7×7 surface ($[11\bar{2}]$ incidence), (d) 1.7-ML-Au adsorption onto (c), and (e) the 5×2 -Au surface before the Au deposition.

structure [14]. The Fermi level is so strongly pinned at the state that the band bending scarcely changes with adsorption of metal atoms, resulting in small changes in conductance at the beginning of metal deposition onto the 7×7 surface [Figs. 2(a) and 4(a)].

Taking into account the fact that the Si(111)- $\sqrt{3}\times\sqrt{3}$ -Ag surface is "semiconducting" [15], the Fermi level at the surface is expected to easily shift with the subsequent Ag adsorption. Since the Ag adatoms act as

donors, the band will bend downwards to increase the concentration of conduction electrons near the surface. A very small amount of Ag adatoms is enough to cause such variation, resulting in an abrupt decrease in resistance at the beginning in Fig. 2(b).

Since photoemission data [16] indicate that the bands at the 5×2 -Au surface initially bend upwards strongly enough to create a *p*-type inversion layer due to acceptor-like surface states, the great increase in resistance in Fig. 4(b) is understood as follows: The "pinning force" for the Fermi level is again weak, so that Au adsorption onto this surface makes the bands bend downwards because of the donorlike action of the Au adatoms. This means a decrease of the hole concentration in the space-charge region. After reaching the minimum surface conductance of a depletion layer, the surface will convert to an *n*-type accumulation layer for the duration of the deposition and turn to a decrease in resistance.

With increase of the metal coverage, the conduction through the grown metal film may dominate the resistance changes, the effect of which strongly depends on the epitaxial growth mechanism. The rates of decrease in resistance during Ag deposition in the thicker coverage region (more than 3 ML) were quite different between Figs. 2(a) and 2(b). This seems to support the simple expectation that 2D Ag islands on the surface more easily create percolation paths than 3D Ag nuclei. The thick Au films, on the other hand, seem similar in structure, irrespective of the initial substrate surface, resulting in almost equal rates of decrease in resistance with Au coverage.

In situ measurements like the present study will not only provide valuable insight into the fundamental understanding of surface and interface phenomena such as Schottky-barrier formation, but will also lead to industrial applications. Further results and detailed discussions with photoemission data will be given in a more extended paper.

The present study was supported in part by a Grant-In-Aid from the Ministry of Education, Science and Culture of Japan, and also by the Murata Science Foundation.

- [1] For example, J. C. Rivière, *Surface Analytical Techniques* (Clarendon, Oxford, 1990); in *Reflection High-Energy Electron Diffraction and Reflection Electron Imaging of Surfaces*, edited by P. K. Larson and P. J. Dobson (Plenum, New York, 1988).
- [2] L. J. Brillson, *Surf. Sci. Rep.* **2**, 123 (1982).
- [3] A. Many, Y. Goldstein, and N. B. Grover, *Semiconductor Surfaces* (North-Holland, Amsterdam, 1965); D. R. Frankl, *Electrical Properties of Semiconductor Surfaces* (Pergamon, Oxford, 1967); in *Metallization and Metal-Semiconductor Interfaces*, edited by I. P. Batra (Plenum, New York, 1988).
- [4] R. T. Tung, *Phys. Rev. Lett.* **52**, 461 (1984).
- [5] D. R. Heslinga *et al.*, *Phys. Rev. Lett.* **64**, 1589 (1990).
- [6] M. Jałochowski and E. Bauer, *Phys. Rev. B* **37**, 8622 (1988); **38**, 5272 (1988); *Surf. Sci.* **213**, 556 (1989).
- [7] F. G. Allen and G. W. Gobell, *Phys. Rev.* **144**, 558 (1966); W. Mönch, *Phys. Status Solidi* **40**, 257 (1970); L. He and H. Yasunaga, *Jpn. J. Appl. Phys.* **24**, 928 (1985); L. Surnev and M. Tikhov, *Surf. Sci.* **85**, 413 (1979).
- [8] H. J. W. Zandvliet and A. Van Silfhout, *Surf. Sci.* **195**, 138 (1988); L. Surnev and M. Tikhov, *Surf. Sci.* **138**, 40 (1984).
- [9] Y. Gotoh and S. Ino, *Jpn. J. Appl. Phys.* **17**, 2097 (1978); *Thin Solid Films* **109**, 255 (1983); *J. Cryst. Growth* **56**, 498 (1982).
- [10] S. Hasegawa, H. Daimon, and S. Ino, *Surf. Sci.* **186**, 138 (1987); M. Katayama *et al.*, *Phys. Rev. Lett.* **66**, 2762 (1991); T. Takahashi *et al.*, *Jpn. J. Appl. Phys.* **27**, L753 (1988).
- [11] G. LeLay *et al.*, *Thin Solid Films* **35**, 273 (1976).
- [12] S. Ino, *J. Phys. Soc. Jpn.* **37**, 82 (1982); *Jpn. J. Appl. Phys.* **16**, 891 (1977); H. Daimon *et al.*, *Surf. Sci.* **235**, 142 (1990); S. Takahashi *et al.*, *Surf. Sci.* **242**, 73 (1991); Y. Tanishiro, K. Yagi, and K. Takayanagi, *Surf. Sci.* **234**, 37 (1990); A. A. Baski, J. Nogami, and C. F. Quate, *Phys. Rev. B* **41**, 247 (1990).
- [13] R. J. Hamers, R. M. Tromp, and J. E. Demuth, *Phys. Rev. Lett.* **56**, 1972 (1986).
- [14] K. Takayanagi *et al.*, *J. Vac. Sci. Technol. A* **3**, 1502 (1985); *Surf. Sci.* **164**, 367 (1985).
- [15] T. Yokotsuka *et al.*, *Surf. Sci.* **127**, 35 (1983); J. M. Nicholls, F. Salvan, and B. Reihl, *Phys. Rev. B* **34**, 2945 (1986).
- [16] H. Daimon, Y. Tezuka, and S. Ino (to be published).

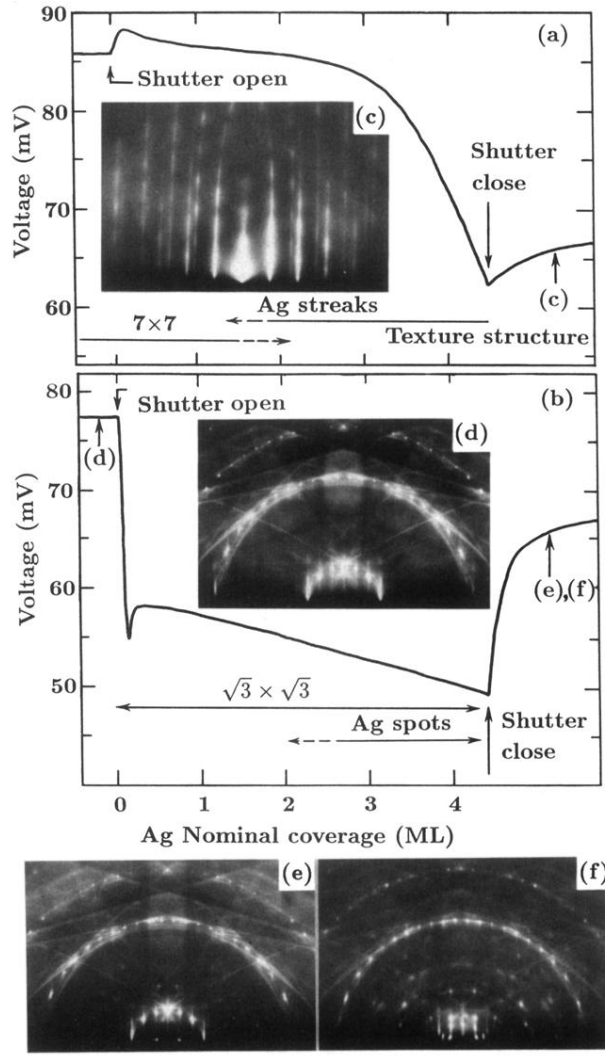


FIG. 2. The resistance changes during the room-temperature Ag depositions onto (a) clean Si(111)- 7×7 and (b) Si(111)- $\sqrt{3}\times\sqrt{3}$ -Ag surfaces. RHEED patterns are shown as insets: (c) a texture structure after 4.5-ML-Ag deposition on the 7×7 surface ($[1\bar{1}0]$ incidence); $\sqrt{3}\times\sqrt{3}$ -Ag substrate (d) before the Ag deposition ($[1\bar{1}\bar{2}]$ incidence), (e) after 4.5-ML-Ag deposition onto (d), and (f) small glancing-angle observation of (e).

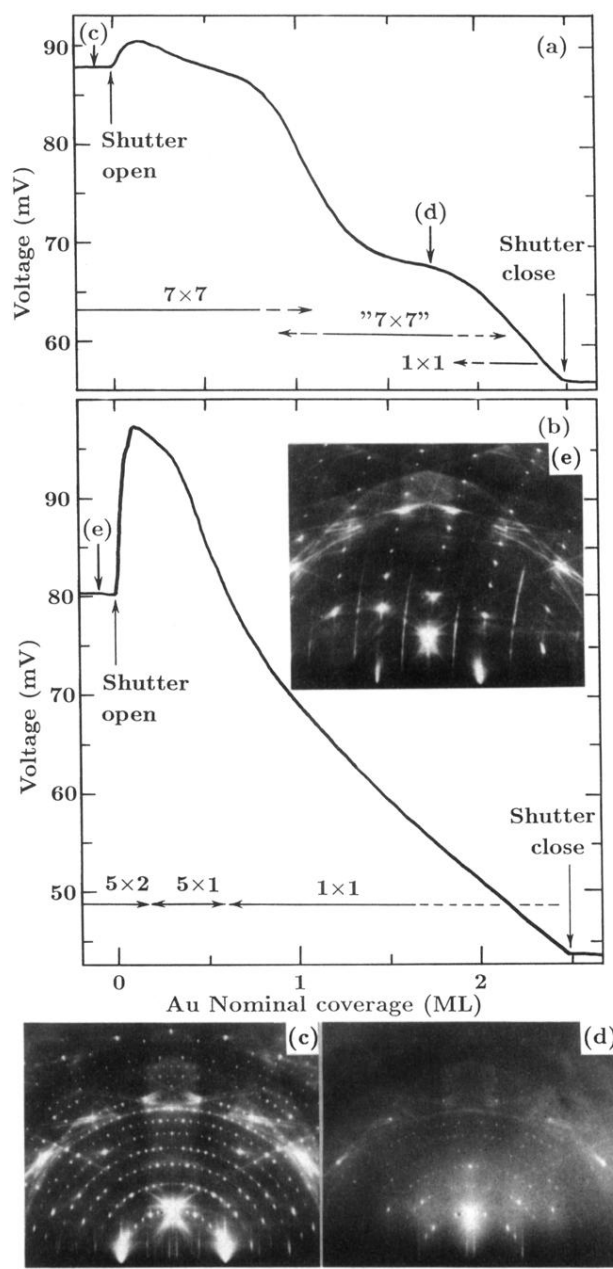


FIG. 4. The resistance changes during the room-temperature Au depositions onto (a) clean Si(111)-7x7 and (b) Si(111)-5x2-Au surfaces. RHEED patterns are shown as insets: (c) the clean 7x7 surface ($[11\bar{2}]$ incidence), (d) 1.7-ML-Au adsorption onto (c), and (e) the 5x2-Au surface before the Au deposition.